Structure and vibrational dynamics of isotopically labeled lithium borohydride using neutron diffraction and spectroscopy

Michael R. Hartman[a],*, John J. Rush[a], Terrence J. Udovic[a],
Robert C. Bowman Jr.[b], Son-Jong Hwang[c]

[a]NIST Center for Neutron Research, National Institute of Standards and Technology, Gaithersburg, MD 20899-8562, USA
[b]Jet Propulsion Laboratory, California Institute of Technology, Pasadena, CA 91109, USA
[c]Division of Chemistry and Chemical Engineering, California Institute of Technology, Pasadena, CA 91125, USA

Abstract

The crystalline structure of a ^{7}Li and ^{11}B labeled lithium borohydride has been investigated using neutron powder diffraction at 3.5, 360, and 400 K. The B–H bond lengths and H–B–H angles for the $[BH_4]^-$ tetrahedra indicated that the tetrahedra maintained a nearly ideal configuration throughout the temperature range investigated. The atomic displacement parameters at 360 K suggest that the $[BH_4]^-$ tetrahedra become increasingly disordered as a result of large amplitude librational and reorientational motions as the orthorhombic to hexagonal phase transition ($T = 384$ K) is approached. In the high-temperature hexagonal phase, the $[BH_4]^-$ tetrahedra displayed extreme disorder about the trigonal axis along which they are aligned. Neutron vibrational spectroscopy data were collected at 5 K over an energy range of 10–170 meV, and were found to be in good agreement with prior Raman and low-resolution neutron spectroscopy studies.
© 2007 Elsevier Inc. All rights reserved.

Keywords: Neutron scattering; Lithium borohydride; NMR; Hydrogen storage

1. Introduction

The successful implementation of a hydrogen economy is critically dependent upon the development of hydrogen storage systems with high volumetric and gravimetric storage densities that operate at temperatures and pressures consistent with fuel cell applications. Lithium borohydride ($LiBH_4$) is an attractive solid state hydrogen storage material with volumetric and gravimetric storage densities of 122 kg H/m^3 and 18.5 mass percent H, respectively, and several research groups have recently explored reversible hydrogen storage in $LiBH_4$ by the inclusion of catalytic or destabilizing additives [1–3].

Lithium borohydride is not a new material. Indeed, its synthesis was first reported more than 60 years ago [4], and since its discovery, it has played an important role as a selective reducing agent in organometallic chemistry. The structure of $LiBH_4$ was first investigated by Harris and Meibohm using X-ray diffraction (XRD) and more recently by Soulié et al. with synchrotron XRD [5,6]. The results of the synchrotron investigation showed that at low-temperatures, the material crystallized in an orthorhombic structure and underwent a first-order phase transition to a hexagonal structure at ∼381 K. Refinement of the XRD data suggested that the $[BH_4]^-$ tetrahedra in the low-temperature phase were severely distorted with B–H bond lengths ranging from 1.04(2) to 1.28(1) Å and H–B–H angles ranging from 85.1° to 120.1°. The large atomic displacement parameters observed in the high-temperature hexagonal phase suggested reorientational motion of the $[BH_4]^-$ tetrahedra, consistent with the observation of prior Raman and NMR studies, which noted dynamical motion of the tetrahedra [7,8]. Neutron scattering techniques, because of their inherent sensitivity to hydrogen and its
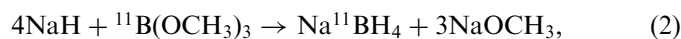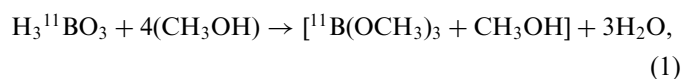
*Corresponding author. Oregon State University, 100 Radiation Center, Corvallis, OR 97331-5903, USA. Fax: +1 541 737 0480.
E-mail address: mike.hartman@oregonstate.edu (M.R. Hartman).

isotopes, have the potential to add important structural and spectroscopic information to these studies, but to date they have not been practical due to the high neutron absorption cross sections associated with naturally occurring Li and B. In the present study, we report the synthesis and characterization of an isotopically labeled lithium borohydride (^{7}Li^{11}BH$_4$), which overcomes the neutron absorption issue and permits the application of powerful neutron scattering techniques. To gain further insight into the structure and dynamics of LiBH$_4$, the isotopically labeled material was studied by neutron powder diffraction and neutron vibrational spectroscopy.

2. Experimental

The synthesis of the isotopically labeled lithium borohydride utilized ^{7}Li and ^{11}B enriched reactants and employed previously documented synthesis pathways [9–11], with the overall chemical reaction given as follows:

$$H_3{}^{11}BO_3 + 4(CH_3OH) \rightarrow [{}^{11}B(OCH_3)_3 + CH_3OH] + 3H_2O, \tag{1}$$

$$4NaH + {}^{11}B(OCH_3)_3 \rightarrow Na^{11}BH_4 + 3NaOCH_3, \tag{2}$$

$$Na^{11}BH_4 + {}^{7}LiCl \rightarrow {}^{7}Li^{11}BH_4 + NaCl. \tag{3}$$

Due to the extreme sensitivity of both sodium borohydride (NaBH$_4$) and LiBH$_4$ to atmospheric moisture, all syntheses were performed using air-sensitive chemistry techniques [12]. Glassware was thoroughly washed, rinsed with deionized water, dried for approximately 12 h at 413 K, and assembled hot under a dry nitrogen purge. Syntheses were performed under an overpressure of dry nitrogen with the exhaust routed through a mineral oil bubbler. Transfer of liquid reactants or products was accomplished using double-ended needles, and manipulation of powdered material was performed in either a helium or nitrogen filled glove box. The ^{11}B enriched boric acid utilized in reaction 1 was obtained from Sigma-Aldrich (Boric Acid-^{11}B, 99 at% ^{11}B) [13]. The ^{11}B enriched trimethyl borate azeotrope, shown in reaction 1, was separated using a fractional distillation column, and the trimethyl borate was separated from its azeotrope by the addition of lithium chloride (LiCl) [9]. The reaction to produce the ^{11}B enriched NaBH$_4$, as detailed in reaction 2, was conducted at 250 °C using a jacketed reaction vessel connected to a silicone oil bath. The ^{11}B enriched NaBH$_4$ was extracted from other reaction products by dissolution in isopropylamine. Following recrystallization in the isopropylamine, the Na^{11}BH$_4$ was further purified by an additional extraction and recrystallization in diethylene glycol dimethyl ether. Reaction 3 utilized the purified Na^{11}BH$_4$ from reaction 2 along with ^{7}Li enriched LiCl from Isotec (Lithium-^{7}Li Chloride, 99 at% ^{7}Li) [13]. The reaction was conducted in isopropylamine under reflux conditions. Following the reaction, the soluble ^{7}Li^{11}BH$_4$ was extracted from the insoluble sodium chloride, and the

isopropylamine was removed under active evacuation at 373 K. A further extraction and recrystallization in diethyl ether was used to purify the ^{7}Li^{11}BH$_4$. Characterization of the reactants and products throughout the various reaction processes was performed using XRD and infrared spectroscopy [13–15]. In addition, the ^{7}Li^{11}BH$_4$ was further characterized using ^{1}H, ^{7}Li, and ^{11}B NMR spectroscopy. The solid state magic angle spinning nuclear magnetic resonance (MAS-NMR) measurements were performed using a Bruker Avance 500 MHz spectrometer [13] with a wide bore 11.7 T magnet and using a Bruker 4 mm MAS probe. The samples were packed into a 4-mm ZrO$_2$ rotor in an argon atmosphere glove box and sealed with a tight fitting Kel-F cap. Dry nitrogen gas was used for sample spinning. All MAS-NMR experiments were performed at room temperature.

Neutron powder diffraction (NPD) studies were conducted on the high resolution neutron powder diffractometer (BT-1) at the NIST Center for Neutron Research (NCNR). Due to the large incoherent neutron scattering cross section of hydrogen, the sample utilized in the NPD measurements was deuterated by exposing it to gaseous deuterium at a pressure of ~7.5 bar and a temperature of 473 K over a two-week period. Following the deuteration, 226 mg of the ^{7}Li^{11}BD$_4$ material was loaded into a vanadium sample cell and sealed with a press-fit indium gasket. NPD data were collected over an angular range of $5.0° \leqslant 2\theta \leqslant 150.0°$ with a step size of $0.05°$ at temperatures of 3.5, 360, and 400 K and an incident neutron wavelength of 1.5403 Å. The data were subjected to Rietveld refinement using the GSAS code as implemented in EXPGUI [16,17].

Neutron vibrational spectroscopy (NVS) data were collected with the Filter-Analyzer Neutron Spectrometer (FANS) at the NCNR [18]. The NVS technique takes advantage of the large incoherent scattering cross section of hydrogen, hence ^{7}Li^{11}BH$_4$ was used without deuteration. The 154 mg sample of ^{7}Li^{11}BH$_4$ was contained in an aluminum sample cell and sealed with a press-fit indium gasket. NVS data were collected at 5 K with an incident neutron energy ranging from 10 to 170 meV and a fixed final energy of 1.2 meV. In-pile and post-monochromator collimations of 20 min of arc were used.

3. Results and discussion

The ^{7}Li and ^{11}B enriched lithium borohydride produced by the described synthesis process exhibited XRD, infrared, and NMR features that were consistent with those of a commercial LiBH$_4$ composed of the natural isotopic abundances of Li and B. The ^{7}Li and ^{11}B contents were both estimated to be >99 at%, based upon the enrichment of the reactants, and no crystalline impurity phases could be identified in the XRD data. The ^{7}Li^{11}BH$_4$ was obtained as a finely divided white powder.

The ^{11}B and ^{1}H MAS-NMR spectra for the ^{7}Li^{11}BH$_4$ material are compared in Fig. 1 to spectra for commercial

LiBH$_4$ from Alfa-Aesar [13] with natural isotopic abundances. While slightly higher levels of impurity contents are seen in these ^{1}H and ^{11}B spectra for ^{7}Li^{11}BH$_4$, which are probably B$_2$O$_3$ or B(OH)$_3$ related phases plus perhaps some elemental boron; no significant differences are observed for the enriched material that may be correlated with structural distortion. From rough relative peak areas for impurity species and relative sample weights, the impurity contents are 4–5 times larger in the NIST sample, but still only about 1–2% of total phase composition. The
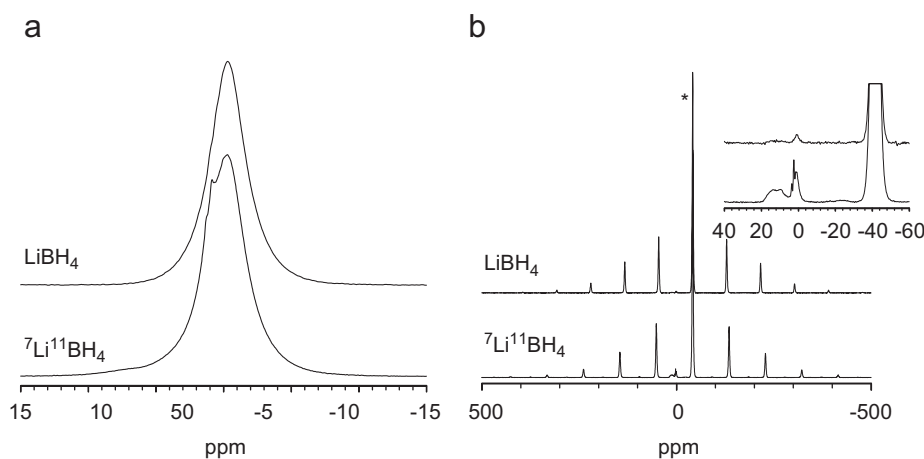

Fig. 1. ^{1}H and ^{11}B MAS NMR spectra of synthesized ^{7}Li^{11}BH$_4$ sample plotted together with those for natural isotopic abundance LiBH$_4$ from Alfa-Aesar. (a) ^{1}H MAS NMR spectra where the borohydride peak occurs at −0.3 ppm (only center band is shown) and the shoulder at ∼1 ppm for the labeled ^{7}Li^{11}BH$_4$ sample (lower curve) is probably from impurities such as B(OH)$_3$. (b) ^{11}B MAS NMR spectra of ^{7}Li^{11}BH$_4$ and the commercial borohydride. The expanded view is inserted to show low level peaks with shifts in the range ∼0–20 ppm from impurities. The main peak for the BH$_4^-$ species in the two borohydride samples, as denoted by the asterisk, occurs at −41.3 ppm for the central transition (−1/2↔1/2) of ^{11}B ($I = 3/2$). The remainder of the sharp peaks are spinning sidebands which extend over approximately an 800 ppm range and are attributed to the satellite transitions.

Table 1
Summary of Rietveld refinement of the ^{7}Li^{11}BD$_4$ NPD data at 3.5 K

Space group	Pnma (no. 62)				
Sample temperature (K)	3.5 K				
Lattice parameter (Å)					
a	7.1213 (2)				
b	4.4060 (1)				
c	6.6744 (2)				
R_{wp}	2.70%				
R_p	2.21%				
χ^2	0.9037				
Durbin–Watson statistic, d	1.383				
Atom	Site	x	y	z	Fractional occupation
Li	4c	0.1597 (10)	1/4	0.1106 (10)	1
B	4c	0.3054 (3)	1/4	0.4301 (5)	1
H1	4c	0.4072 (6)	1/4	0.5759 (10)	1
H2	4c	0.3995 (6)	1/4	0.2766 (6)	1
H3	8d	0.2048 (4)	0.0293 (5)	0.4268 (7)	1

Atomic displacement parameters ($U_{ij} * 100$) (Å^2)

Atom	U_{11}	U_{22}	U_{33}	U_{12}	U_{13}	U_{23}
Li	0.74 (35)	1.76 (33)	2.17 (49)	0	−0.41 (25)	0
B	1.02 (13)	0.24 (10)	1.52 (13)	0	−0.07 (16)	0
H1	2.12 (22)	1.86 (19)	0.80 (19)	0	0.21 (24)	0
H2	1.02 (26)	3.44 (26)	0.94 (23)	0	0.39 (19)	0
H3	3.08 (18)	1.75 (13)	2.78 (17)	−0.45 (14)	0.33 (23)	0.22 (17)

Estimated standard deviations are shown in parentheses.

Table 2
Summary of Rietveld refinement of the $^7\mathrm{Li}^{11}\mathrm{BD}_4$ NPD data at 360 K

Space group	*Pnma* (no. 62)
Sample temperature (K)	360 K
Lattice Parameter (Å)	
a	7.1914 (5)
b	4.4256 (3)
c	6.8641 (4)
R_{wp}	2.53%
R_p	2.13%
χ^2	0.7850
Durbin–Watson statistic, *d*	1.549

Atom	Site	*x*	*y*	*z*	Fractional occupation
Li	4*c*	0.1651 (24)	1/4	0.1082 (22)	1
B	4*c*	0.2987 (9)	1/4	0.4288 (10)	1
H1	4*c*	0.3973 (17)	1/4	0.5670 (22)	1
H2	4*c*	0.3972 (22)	1/4	0.2846 (19)	1
H3	8*d*	0.1989 (11)	0.0372 (15)	0.4270 (16)	1

Atomic displacement parameters ($U_{ij}*100$) (Å^2)

Atom	U_{11}	U_{22}	U_{33}	U_{12}	U_{13}	U_{23}
Li	7.6 (15)	4.5 (10)	3.4 (10)	0	−0.46 (71)	0
B	6.1 (4)	4.3 (3)	4.5 (3)	0	−0.94 (43)	0
H1	8.1 (8)	9.5 (8)	5.9 (6)	0	1.2 (9)	0
H2	8.7 (13)	19.2 (15)	4.9 (7)	0	2.5 (9)	0
H3	8.6 (7)	8.9 (6)	14.2 (8)	−3.8 (6)	−4.4 (7)	3.2 (7)

Estimated standard deviations are shown in parentheses.

Table 3
Summary of Rietveld refinement of the $^7\mathrm{Li}^{11}\mathrm{BD}_4$ NPD data at 400 K

Space group	*P6₃mc* (no. 186)
Sample temperature (K)	400 K
Lattice parameter (Å)	
a	4.2667 (2)
c	6.9223 (8)
R_{wp}	2.59%
R_p	2.15%
χ^2	0.8284
Durbin–Watson statistic, *d*	1.419

Atom	Site	*x*	*y*	*z*	Fractional occupation
Li	2*b*	1/3	2/3	0	1
B	2*b*	1/3	2/3	0.5756 (40)	1
H1	2*b*	1/3	2/3	0.4366 (104)	1
H2	6*c*	0.2053 (18)	0.4106 (36)	0.6321 (68)	1

Atomic displacement parameters ($U_{ij}*100$) (Å^2)

Atom	U_{11}	U_{22}	U_{33}	U_{12}	U_{13}	U_{23}
Li	6.1 (10)	6.1 (10)	6.1 (44)	1.3 (5)	0	0
B	6.8 (4)	6.8 (4)	15 (3)	3.4 (2)	0	0
H1	64 (11)	64 (11)	7.4 (46)	40 (5)	0	0
H2	16 (1)	9.2 (9)	43 (4)	4.6 (4)	6.4 (10)	13 (2)

Estimated standard deviations are shown in parentheses.

"elemental boron" peaks for both $LiBH_4$ samples is much sharper than the peak for crystalline elemental boron powder, suggesting less disorder for the impurities in the borohydrides. ^{7}Li MAS NMR spectra (not shown) of the labeled material exhibited mainly the central band (fwhm ~250 Hz) at −1.1 ppm due to minor contribution of quadrupole coupling, and was practically indistinguishable from that of unlabeled material.

To account for the isotopic substitution, the Rietveld refinement of the NPD data used neutron scattering

Table 4
Observed and corrected B–H bond distances within the $[BH_4]^-$ tetrahedra for synchrotron X-ray and NPD studies

Source of data	B–H bond description	Observed bond length from Rietveld refinement (Å)	Bond length corrected for proton riding motion (Å)
Low-temperature *Pnma* phase:			
Synchrotron X-ray data at 293 K (Ref. [6])	B–H1	1.04(2)	1.06(2)
	B–H2	1.25(1)	1.27(1)
	B–H3	1.28(1)	1.31(1)
	Avg. B–H	1.21(2)	1.24(1)
NPD from this work at 3.5 K	B–H1	1.213(7)	1.221(7)
	B–H2	1.225(6)	1.238(5)
	B–H3	1.208(3)	1.223(3)
	Avg. B–H	1.214(5)	1.226(5)
NPD from this work at 360 K	B–H1	1.184(16)	1.197(16)
	B–H2	1.217(15)	1.299(17)
	B–H3	1.184(7)	1.254(9)
	Avg. B–H	1.192(11)	1.251(13)
High-temperature *P6₃mc* phase:			
Synchrotron X-ray data at 408 K (Ref. [6])	B–H1	1.27(2)	1.22(2)
	B–H2	1.29(2)	1.53(3)
	Avg. B–H	1.29(2)	1.45(3)
NPD from this work at 400 K	B–H1	0.9621(1)	1.56(14)
	B–H2	1.02414(4)	1.23(10)
	Avg. B–H	1.0086(1)	1.31(11)

Estimated standard deviations are shown in parentheses.
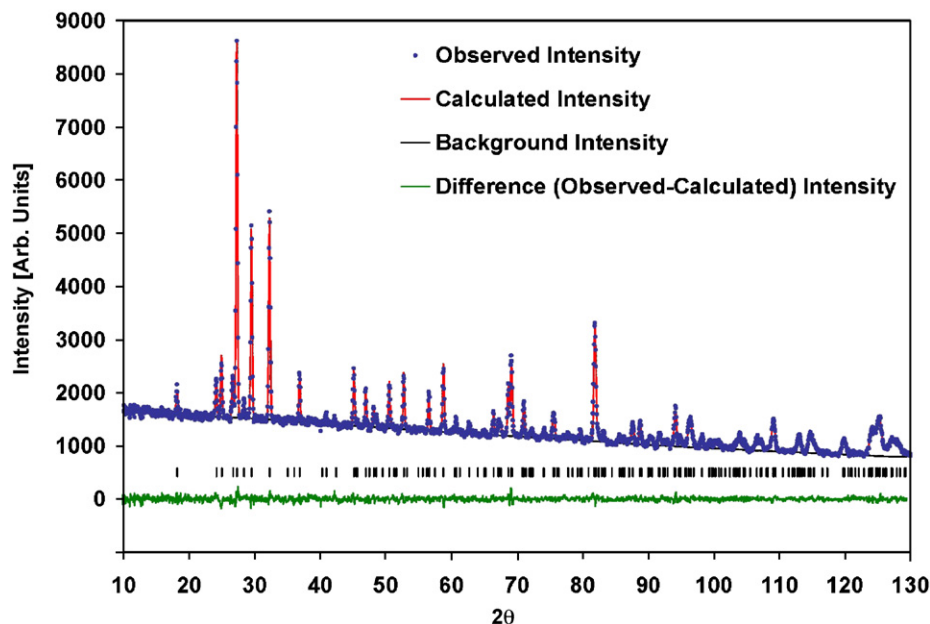
Fig. 2. Results of the Rietveld refinement of the [7]Li[11]BD_4 NPD data at 3.5 K.

lengths of −2.22 and 6.65 fm for [7]Li and [11]B, respectively. The neutron scattering length for the deuterium present at the hydrogen atomic sites was set to 4.16 fm to account for a partial deuteration of ∼76% in the sample used for the NPD. The deuteration fraction was determined by an initial Rietveld refinement of the diffraction data at 3.5 K.

The results of the Rietveld refinements of the NPD data, collected at 3.5, 360, and 400 K, are summarized in Tables 1–3, respectively. The B–H bond lengths observed from the Rietveld refinements along with the bond lengths corrected for a riding motion of the hydrogen atoms on the central boron atom, using the formalism of Busing and Levy [19], for both the synchrotron XRD study of Soulié et al. [6] and the current NPD investigation are summarized in Table 4.

The results of the Rietveld refinement for the low-temperature *Pnma* phase at 3.5 K are shown in Fig. 2. The quality of the fit was quite good, and in contrast to the prior synchrotron XRD [6], the geometry of the [BH$_4$]$^-$ tetrahedra that resulted from the refinement had a much more ideal configuration with a mean B–H bond length of 1.226(5) Å and H–B–H angles ranging from 107.2(3)° to 111.7(4)°. This B–H bond length compares favorably with those determined by Renaudin et al. in a recent X-ray and neutron diffraction study of a series of alkali borohydrides [20]. The structure and its associated atomic displacement ellipsoids are shown in Fig. 3.

At 360 K, the structure retained its *Pnma* symmetry, but the atomic displacement ellipsoids associated within the [BH$_4$]$^-$ tetrahedra, depicted in Fig. 3, were much larger than they were at 3.5 K. The increased atomic displacements of the [BH$_4$]$^-$ tetrahedra signifies increased motion of the tetrahedra as a result of librations and dynamical disorder. The mean corrected B–H bond length was 1.251(13) Å and the H–B–H angles ranged from 105.4(9)° to 111.8(8)°.

At 400 K, the Rietveld refinement of the NPD data was performed in the *P6$_3$mc* space group. The resulting crystal structure was similar to that from the synchrotron XRD investigation, with the hydrogen atom coincident with the 3-fold axis, along which the [BH$_4$]$^-$ tetrahedra are aligned, exhibiting large atomic displacement parameters. However, in contrast to the synchrotron XRD investigation, the remaining hydrogen atoms also displayed large atomic displacements. The large atomic displacement parameters associated with the hydrogen atoms in the high-temperature phase, shown in Fig. 4, are consistent with the view that the [BH$_4$]$^-$ tetrahedra are extremely disordered in this phase. The mean corrected B–H bond length of 1.31(11) Å that resulted from the present NPD study is more reasonable than the mean corrected B–H bond length of 1.45(6) Å from the synchrotron XRD investigation, although the very large reorientational displacements make it increasingly difficult to precisely determine B–H bond lengths via the Busing–Levy correction.

The NVS data collected for the [7]Li[11]BH$_4$ at 5 K are shown in Fig. 5. The present study employed a

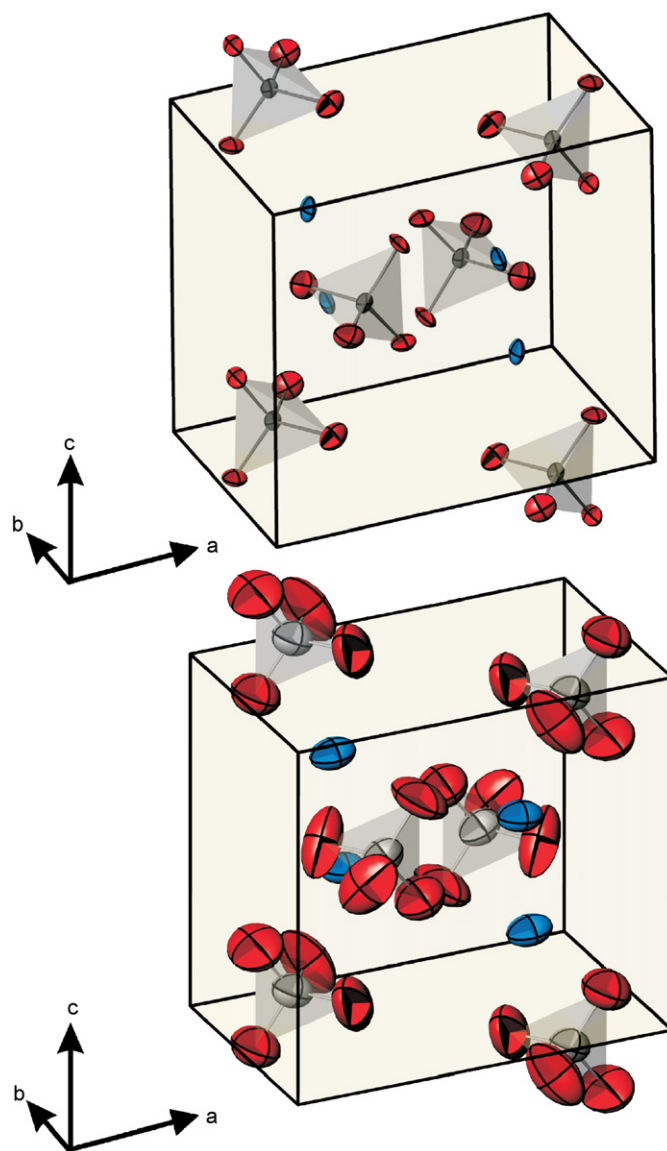Fig. 3. Comparison of the structure of [7]Li[11]BH$_4$ in the low-temperature *Pnma* phase, including atomic displacement ellipsoids, at 3.5 K (top) and 360 K (bottom). Boron atoms are at the center of the tetrahedral structures with hydrogen atoms located at the apices. Lithium ions are distributed between the [BH$_4$]$^-$ tetrahedra.

spectrometer with an improved energy resolution as compared to the work of Tomkinson and Waddington [21] and provided complementary information for comparison to recent Raman studies [7,22]. The NVS data show features from ∼20 to 35 meV that are attributed to translatory lattice modes of [7]Li[11]BH$_4$. Also visible is the [BH$_4$]$^-$ librational mode, v_L, at ∼52 meV. The width of the librational mode is far in excess of the instrumental resolution (∼1.3 meV at the position of the librational mode) and suggests the presence of multiple, unresolved features. Two internal [BH$_4$]$^-$ vibrational modes, v_2 and v_4, were also observed and were found to be in good agreement with those determined by Gomes et al. using Raman spectroscopy [22].
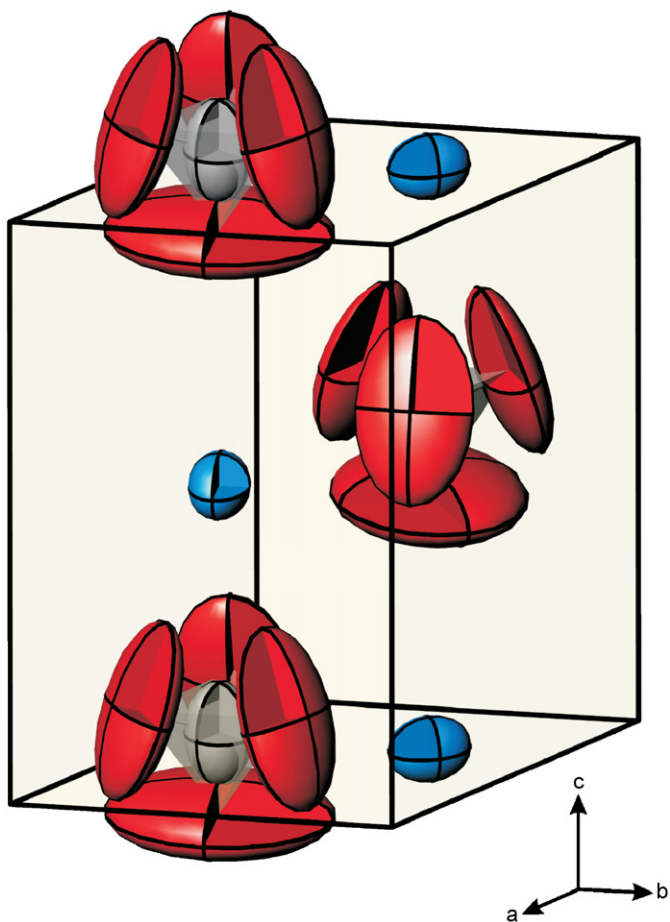
Fig. 4. Structure of $^7Li^{11}BH_4$ in the high-temperature $P6_3mc$ phase at 400 K, including atomic displacement ellipsoids. Boron atoms are at the center of the tetrahedral structures with hydrogen atoms located at the apices. Lithium ions are distributed between the $[BH_4]^-$ tetrahedra.

Fig. 5. NVS data for the $^7Li^{11}BH_4$ sample taken at 5 K.

4. Summary and conclusions

A ^7Li and ^{11}B labeled $LiBH_4$ was synthesized to permit structural and dynamical features of the material to be probed with neutron scattering techniques. Neutron powder diffraction in combination with Rietveld refinement confirmed the space group assignments of Soulié et al. [6] based upon synchrotron XRD data. However, in contrast to the X-ray study, the $[BH_4]^-$ tetrahedra were found to have a nearly ideal configuration throughout the temperature range investigated.

In the low-temperature *Pnma* phase, NPD data were collected at 3.5 and 360 K. The mean B–H distance, corrected for atomic displacement, at 3.5 K was observed to be 1.226(5) Å, while at 360 K a value of 1.251(13) Å was determined. The increased atomic displacement parameters associated with the crystalline structure at 360 K suggested that large amplitude librations and reorientational motions were present well below the structural transition at 384 K. Refinement of the high-temperature hexagonal phase yielded a mean B–H bond length of 1.31(11) Å and exhibited extremely large atomic displacement parameters
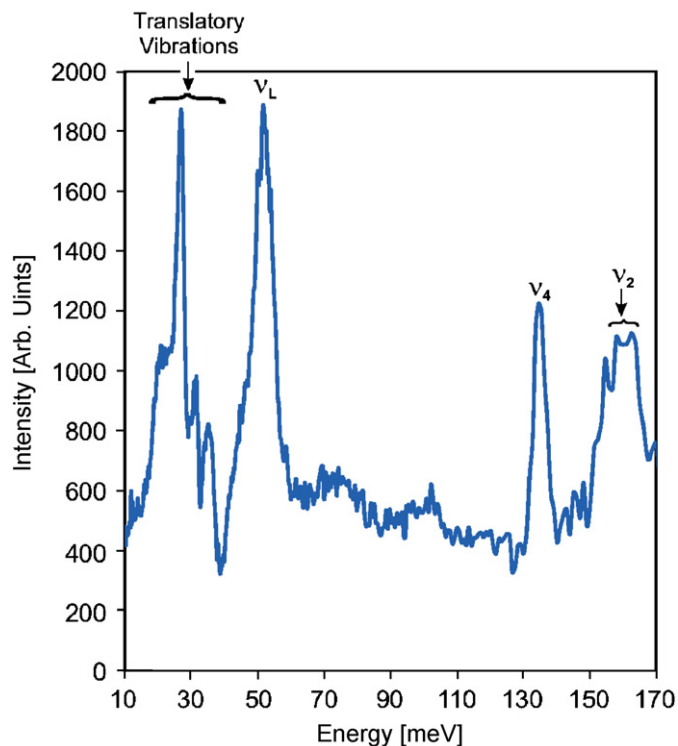
for the hydrogen atoms associated with the $[BH_4]^-$ tetrahedra, indicative of severe disorder of the tetrahedra in the high-temperature phase.

The vibrational spectra of lithium borohydride were probed with NVS. The measurements extended the range of prior NVS measurements and corroborated internal mode frequencies assigned by Raman spectroscopy.

References

[1] A. Züttel, P. Wenger, S. Rentsch, P. Sudan, Ph. Mauron, Ch. Emmenegger, J. Power Sources 118 (2003) 1–7.
[2] Y. Nakamori, S. Orimo, J. Alloy Compd. 370 (2004) 271–275.
[3] J. Vajo, S. Skeith, F. Mertens, J. Phys. Chem. B 109 (2005) 3719–3722.
[4] H.I. Schlesinger, H.C. Brown, J. Am. Chem. Soc. 62 (1940) 3429–3435.
[5] P.M. Harris, E.P. Meibohm, J. Am. Chem. Soc. 69 (1947) 1231–1232.

[6] J.-Ph. Soulié, G. Renaudin, R. Černý, K. Yvon, J. Alloy Compd. 346 (2002) 200–205.

[7] H. Hagemann, S. Gomes, G. Renaudin, K. Yvon, J. Alloy Compd. 363 (2004) 126–129.

[8] T. Tsang, T.C. Farrar, J. Chem. Phys. 50 (1969) 3498–3502.

[9] H.I. Schlesinger, H.C. Brown, D.L. Mayfield, J.R. Gilbreath, J. Am. Chem. Soc. 75 (1953) 213–215.

[10] H.I. Schlesinger, H.C. Brown, A.E. Finholt, J. Am. Chem. Soc. 75 (1953) 205–209.

[11] H.C. Brown, Y.M. Choi, S. Narasimhan, Inorg. Chem. 21 (1982) 3657–3661.

[12] H.C. Brown, Organic Syntheses via Boranes, Wiley, New York, 1975.

[13] Certain commercial firms and trade names are identified in this report in order to specify aspects of the experimental procedure adequately. Such identification is not intended to imply recommendation or endorsement by the National Institute of Standards and Technology, nor is it intended to imply that the materials for equipment identified are necessarily the best available for the purpose.

[14] X-ray diffraction studies were conducted on a Bruker Advanced X-ray Solutions D8 Advance diffractometer using CuKα radiation. Air sensitive materials were sealed in quartz capillaries.

[15] Infrared spectroscopy studies were performed on a Thermo Nicolet Nexus 670 FT-IR Spectrometer.

[16] A.C. Larson, R.B. Von Dreele, General structure analysis system (GSAS), Los Alamos National Laboratory Report LAUR 86–748, 2000.

[17] B.H. Toby, J. Appl. Crystallogr. 34 (2001) 210–213.

[18] T.J. Udovic, D.A. Neumann, J. Leão, C.M. Brown, Nucl. Instrum. Methods Phys. Res. A 517 (2004) 189–201.

[19] W.R. Busing, H.A. Levy, Acta Crystallogr. 17 (1964) 142–146.

[20] G. Renaudin, S. Gomes, H. Hagemann, L. Keller, K. Yvon, J. Alloy Compd. 375 (2004) 98–106.

[21] J. Tomkinson, T.C. Waddington, J. Chem. Soc. Faraday Trans. 72 (1976) 528–538.

[22] S. Gomes, H. Hagemann, K. Yvon, J. Alloy Compd. 346 (2002) 206–210.